Application of Real Time Mid-Infrared FTIR Imaging to Polymeric Systems. 1. Diffusion of Liquid Crystals into Polymers

C. M. Snively and J. L. Koenig*

Department of Macromolecular Science, Case Western Reserve University, Cleveland, Ohio 44106

Received October 15, 1997
Revised Manuscript Received February 10, 1998

Introduction. A variety of analytical techniques have been used to study the diffusion of small molecules in polymers, including radioactive tracer techniques,[1] NMR,[2] and infrared spectroscopy.[3,4] Among the infrared techniques, Fourier transform infrared microspectroscopy[5,6] (FTIRμs) has also been used. FTIRμs is an especially useful technique because, in addition to generating diffusion coefficient data, it can also provide spatially resolved, chemical group specific images which aid in the visualization of the diffusion process.[7,8]

Recent developments in FTIRμs,[9−12] which incorporate focal plane array (FPA) detection,[13] allow the collection of high spatial resolution images of relatively large areas, on the order of 100s of micrometers. Additionally, these data can be acquired in a shorter time than in previous FTIRμs methods: minutes instead of hours. This new method has been used for the analysis of various static biological samples[14,15] and for the analysis of plastic waste.[16] Here, we extend this imaging method to the real-time acquisition of images from systems varying with time. Specifically, we focus on the monitoring of the diffusion of a low molecular weight liquid crystal into a solid polymer film. This particular system is of interest in the study of the phase separation and aging processes in polymer-dispersed liquid crystal display devices.[7,8]

For transmission infrared studies of diffusion, a thin, flat sample geometry must be used. This allows a simplified form of Fick's law to be used.[5,17,18] When combined with Beer's law, the expression for the diffusion profile takes the form of eq 1, where A is the

$$A = \frac{A_0}{2}\,\mathrm{erfc}\left(\frac{x}{2\sqrt{Dt}}\right) \tag{1}$$

absorbance of the diffusant peak at position x along the diffusion direction, A_0 is the absorbance of pure diffusant, erfc is the complimentary error function, D is the concentration independent diffusion coefficient, and t is the diffusion time.

To use eq 1 with previous FTIRμs methods, diffusion is allowed to occur at a temperature above the glass transition temperature, T_g, of the polymer for a certain time. This is necessary because, below this temperature, the polymer is much less mobile, and the diffusion of small molecules through it occurs orders of magnitude slower. The sample is then quenched to below the T_g, which effectively stops the motion of the diffusant and locks in the sample geometry. A series of spectra are acquired along the diffusion direction. The spatially resolved absorbance values of an appropriate diffusant peak along the diffusion direction and the known diffusion time are fitted to eq 1 by a successive approximation method to yield the diffusion coefficient which minimizes the error.

This approach assumes that the diffusion coefficient is concentration independent. In real systems, this is rarely the case.[19] Therefore, to further elucidate the concentration dependence of the diffusion coefficient, several samples must be allowed to diffuse for different times then quenched and examined. This method requires many hours for the collection of high spatial and spectral resolution data.[18]

However, with the new focal plane array imaging method, one sample can be used to acquire images at different times because the collection time is very short, on the order of a few minutes. Overall, multiple images of larger areas with higher spatial resolution can be obtained in less time than one experiment could have been performed using older methods which result in lower spatial resolution and require the preparation of multiple samples. A direct comparison between the two methods therefore cannot be made because the newer method produces data obtained at a spatial resolution not achievable by previous methods. In addition, older methods would take almost 3 days to collect a 64 × 64 pixel spectral image.

Because spatially resolved data are collected at such a fast rate, time-resolved studies of relatively fast processes can be studied in real time. It is useful to define a maximum rate that can be monitored in real time. Any process with a rate faster than this rate cannot be monitored without a spreading out of the spectral data across multiple pixels of the array. This rate can be defined by eq 2, where d is the image

$$R_{\max} = d/t \tag{2}$$

distance corresponding to one pixel and t is the collection time of one image. If the image of the sample changes faster than this rate, spectral data will be spread over multiple pixels, and quantitative information will be lost. With our current instrumentation, it is possible to acquire data for a 64 × 64 pixel image in less than 3 min with a resultant 8 cm^{-1} spectral resolution in the 3950−900 cm^{-1} spectral range. It should again be noted that a direct comparison between this and previous FTIRμs methods cannot be made because comparable spatial resolution cannot be achieved without the use of special techniques such as a synchrotron radiation source[20] or near field techniques.[21]

Experimental Section. The spectrometer used for the acquisition of all data presented here was a Bio-Rad FTS6000 Stingray FTIR imaging spectrometer, which is composed of a UMA500 microscope coupled to an FTS6000 step scan interferometer bench. The detector in this instrument is a Santa Barbara Focal Plane mercury cadmium telluride (MCT) focal plane array detector. This 64 × 64 element detector is capable of detecting radiation in the frequency range of 4000−900 cm^{-1}. A germanium long pass filter was used to block radiation above 3950 cm^{-1} to eliminate Fourier fold-over noise. An additional neutral density filter composed of a 2 mm thick germanium plate was placed immediately before the condensing lens of the optical system to reduce the flux received at the detector. This instru-

S0024-9297(97)01511-8 CCC: $15.00
Published on Web 05/12/1998

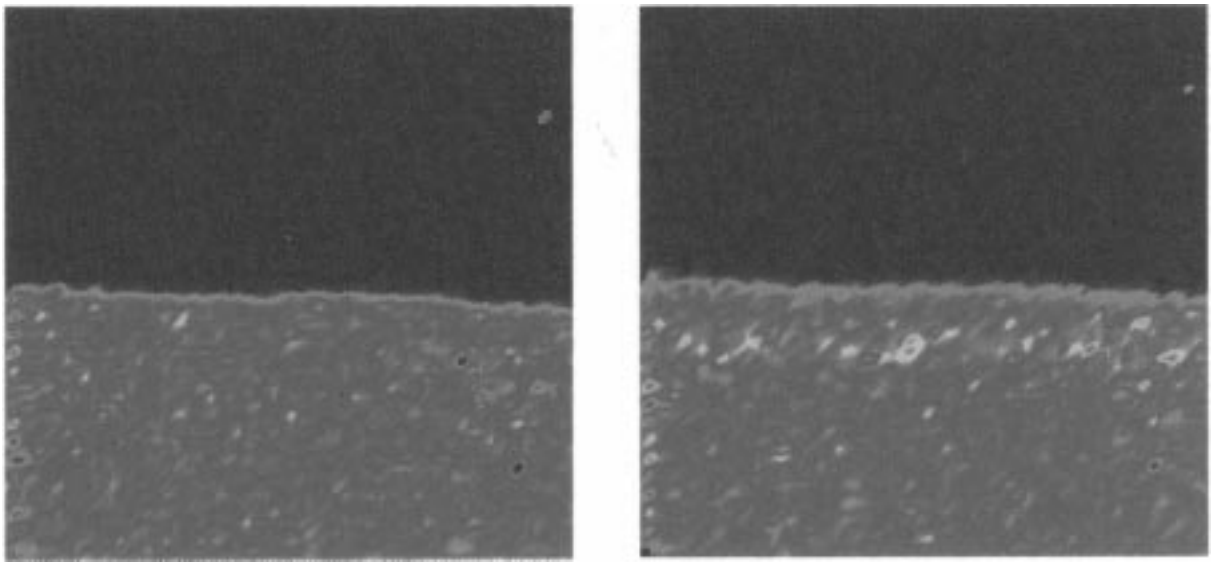

Figure 1. Images of the interface between 5CB and PBMA immediately after contact was made (left) and 1.5 h after contact (right) obtained from the 2227 cm^{-1} band of 5CB. Image size is 64 × 64 pixels, spatial resolution is 8 μm, and spectral resolution is 8 cm^{-1}.

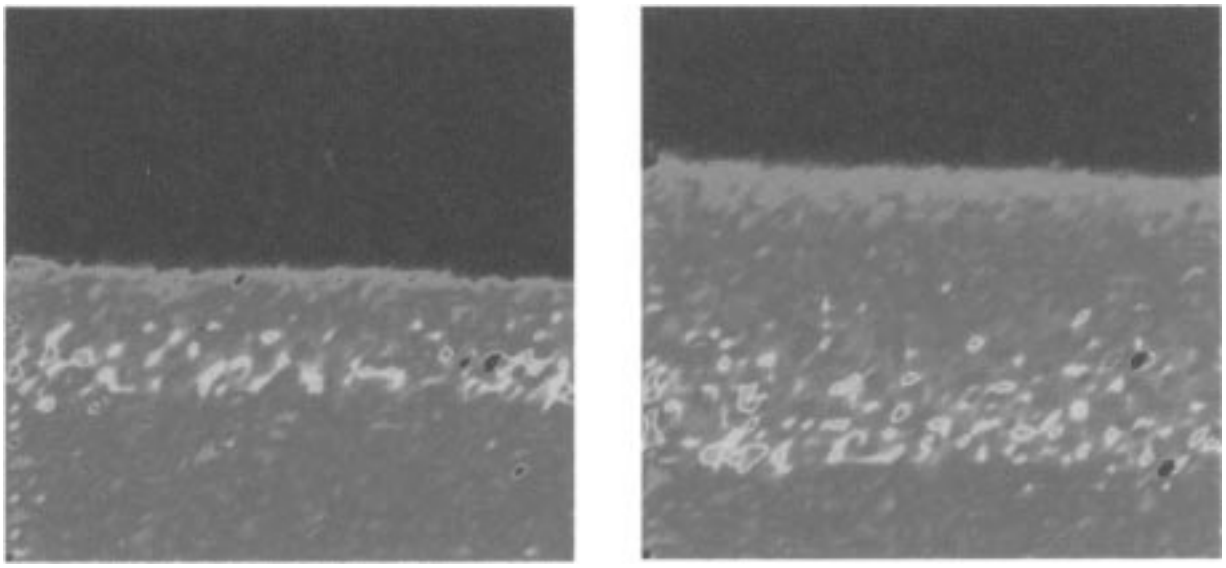

Figure 2. Images of the interface between 5CB and PBMA 3.5 h after contact was made (left) and 20 h after contact (right) obtained from the 2227 cm^{-1} band of 5CB. The same collection parameters as in Figure 1 were used.

mental setup is capable of acquiring spectral images of a 500 × 500 μm region with an average 8 μm spatial (at 2226 cm^{-1}) and 8 cm^{-1} spectral resolution in the 900−3950 cm^{-1} range in slightly less than 3 min.

Poly(butyl methacrylate) (PBMA) from Aldrich and 4-pentyl-4′-cyanobiphenyl (5CB) liquid crystal from EM Industries were used to prepare the samples. These materials were used without further purification. A dilute solution of approximately 10% by weight PBMA in acetone was made. A single droplet of solution was placed on a 1 mm thick zinc selenide (ZnSe) substrate. The solvent was then boiled off with gentle heating. Five micron glass rod spacers were sprinkled around the polymer, and an identical ZnSe plate was placed on top to form a sandwich sample cell geometry. This assembly was placed between two glass slides and held together with a small c-clamp. This assembly was placed in an oven set at 150 °C for 1 h. The sample assembly was then removed, and the c-clamp was tightened further. The assembly was left overnight in the oven to form a thin, uniform film. The samples were then allowed to cool to room temperature. This method produced uniformly thin films of known thickness, as determined from the interference fringe pattern of the resultant spectra.

The sample cell was firmly affixed to the microscope stage via adhesive tape to ensure that the same region was being sampled for each image. A drop of liquid crystal was placed at the edge of the air gap between the cover slips and allowed to move toward the polymer boundary via capillary action. Images were acquired at various times after contact was made between the polymer and liquid crystal. The spectral data was ratioed to an air background and baseline corrected. The absorbance values at the specified frequency were plotted for each detector element in the array to generate the images.

The diffusion coefficient was determined by using a successive approximation method in which the data were plugged into eq 1, and both sides were compared. The diffusion coefficient was varied until the error was minimized for all of the data points.

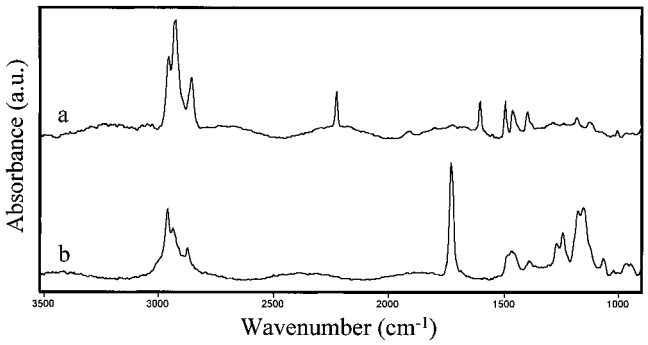

Figure 3. Representative spectra from liquid crystal (a) and polymer (b) regions of the sample.

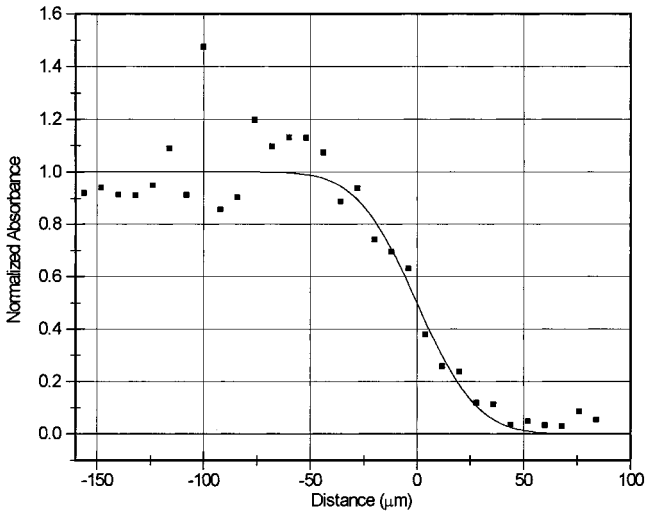

Figure 4. Normalized concentration of the liquid crystal nitrile band across the polymer−liquid crystal interface and ideal Fickian profile.

Results and Discussion. Images acquired immediately after contact between the liquid crystal and polymer and 1.5, 3.5, and 20 h after contact are shown in Figures 1 and 2. These are the result of plotting the absorbance of the 2226 cm^{-1} peak attributed to the CN stretch of the liquid crystal[22] for each of the 4096 pixel positions. The absorbance values are represented by a color scale in which red is the highest intensity and blue is the lowest intensity. From these images, the liquid crystal can be seen to diffuse into the polymer matrix over the span of a few hours.

Representative spectra from the liquid crystal and polymer regions are shown in Figure 3. The signal-to-noise ratios of these spectra are quite good, considering the total array staring time for collection of all 4096 spectra was less than 8 s. The same trading rules are present for this method as are present in standard FTIR spectroscopy. Therefore, the spectral signal-to-noise ratio and resolution can be improved by simply increasing the number of averaged data points. However, as a practical note, each increase in spectral quality requires more collection time, thereby decreasing the maximum attainable temporal resolution.

The diffusion coefficient was determined from the data acquired from a range of diffusion times. These data were processed by methods introduced earlier in this paper. The data are shown in Figure 4, along with the theoretical Fickian diffusion profile corresponding to a diffusion coefficient of $2.5 \times 10^{-10} \pm 0.2 \times 10^{-10}$ $cm^2\ s^{-1}$ (10% error). As can be seen, the measured data fit the theoretical profile remarkably well, except for the point at x position $-$ 100 μm. This point corresponds to the original interface of the film. It is well-known that the optical lensing effect of light rays at the interface of two materials of differing refractive indices (n), such as a thin polymer layer ($n \sim 1.5$) and air ($n \sim 1.0$) causes a decrease in the light intensity received at the detector. This explains why a higher absorbance (lower transmittance) is present in this specific area.

Conclusions. We have shown that FTIR microspectroscopic imaging incorporating focal plane array detection can be used to acquire chemically specific images of diffusion processes in polymeric systems in real time. These images not only aid in the visualization of these processes but also can provide quantitative information about the diffusion processes in the form of diffusion coefficients. This method can be extended to any dynamic process, whether chemical or physical, which occurs at a rate within the real-time detection limit of the system. We are currently using this method to examine the concentration dependence of the diffusion coefficient of this system. We are also extending this method to monitor polymer dissolution and polymer−polymer interdiffusion phenomena.

Acknowledgment. This research was conducted with funding from the National Science Foundation's center for advanced liquid crystalline optical materials (NSF-ALCOM) and the Ohio Board of Regents.

References and Notes

(1) Green, P. F.; et al. *Macromolecules* **1985**, *18*, 501.
(2) Maas, W. E. J. R.; et al. *J. Polym. Sci. B* **1994**, *32*, 785.
(3) Jabbari, E.; Peppas, N. A. *Macromolecules* **1993**, *26*, 2175.
(4) High, M. S.; Painter, P. C.; Coleman, M. M. *Macromolecules* **1992**, *25*, 797.
(5) Cameron, R. E.; Jalil, M. A.; Donald, A. M. *Macromolecules* **1994**, *27*, 2708.
(6) Louden, J. D.; et al. *J. Appl. Polym. Sci.* **1993**, *49*, 275.
(7) Challa, S. R.; Wang, S.-Q.; Koenig, J. L. *Appl. Spectrosc.* **1996**, *50*, 1339.
(8) Challa, S. R.; Wang, S.-Q.; Koenig, J. L. *Appl. Spectrosc.* **1997**, *51*, 10.
(9) Treado, P. J.; Levine, I. W.; Lewis, E. N. *Appl. Spectrosc.* **1994**, *48*, 607.
(10) Lewis, E. N.; Levin, I. W. *Appl. Spectrosc.* **1995**, *49*, 672.
(11) Lewis, E. N.; et al. *Anal. Chem.* **1995**, *67*, 3377.
(12) Lewis, E. N.; et al. *Appl. Spectrosc.* **1997**, *51*, 563.
(13) Scribner, D. A.; Kruer, M. R.; Killany, J. M. *Proc. IEEE* **1991**, *79*, 66.
(14) Lewis, E. N.; et al. *Appl. Spectrosc.* **1996**, *50*, 263.
(15) Hardin, R. W. *Photonics Spectra* **1997**, *31*, 40.
(16) van den Broek, W. H. A. M.; et al. *Appl. Spectrosc.* **1997**, *51*, 856.
(17) Sheu, K.; Huang, S. J.; Johnson, J. F. *Polym. Sci. Eng.* **1989**, *29*, 77.
(18) Sahlin, J. J.; Peppas, N. A. *Macromolecules* **1996**, *29*, 7124.
(19) Vieth, W. R. *Diffusion In and Through Polymers*; Hanser Publishers: New York, 1991.
(20) Meade, C.; Reffner, J. A.; Ito, E. *Science* **1994**, *264*, 1558.
(21) Sahlin, J. J.; Peppas, N. A. *J. Appl. Polym. Sci.* **1997**, *63*, 103.
(22) Snively, C.; et al. *Mol. Cryst. Liq. Cryst., A* **1996**, *289*, 11.

MA971511H